State-of-the-art Temporal Bone Tumour Imaging in Adults

Drs Lee Bo Yee, Li Kwok Yan, Kwok Hoi Ming, Ma Ka Fai Johnny, Cheng Lik Fai
Department of Radiology, Princess Margaret Hospital, Hong Kong SAR

Introduction and Aim:

To illustrate pearls with state-of-the-art imaging techniques in guiding multidisciplinary management in adult temporal bone tumours.

Methods:

Temporal bone tumour cases identified via Radiology Information System of three regional hospitals. Images from Picture Archiving and Communication System.

Results:

Internal Acoustic Meatus (IAM)

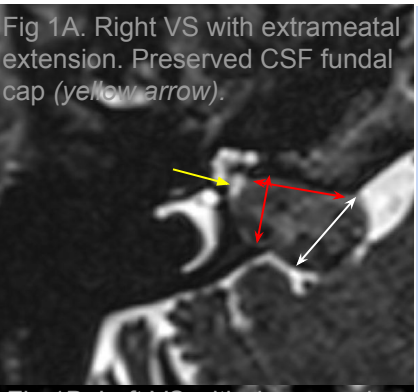

Fig 1A. Right VS with extrameatal extension. Preserved CSF fundal cap *(yellow arrow)*.

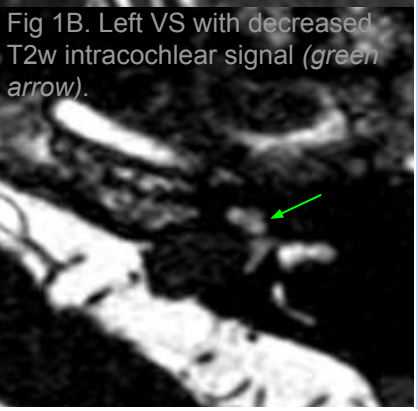

Fig 1B. Left VS with decreased T2w intracochlear signal *(green arrow)*.

Vestibular schwannoma (VS)

- Commonest IAM neoplasm (>90%)
- 95% unilateral. If bilateral, usually associated with neurofibromatosis type II (NF2).
- Classic appearance: Ice-cream cone morphology expanding IAM. Microhaemorrhages and cystic change are common.
- Key tips in reporting:
  - **Size** - separate measurements of extrameatal component (largest extrameatal diameter, *white arrow*) and intrameatal component (length, perpendicular width along IAM, *red arrows*)
  - **Cystic spaces** - faster growth rate, reduced radiosurgery efficacy, and higher morbidity from microsurgery
  - **CSF fundal cap** *(yellow arrow)* - better hearing outcome after surgery, lower risk of facial nerve injury if preserved
  - **Change in intracochlear signal** - decreased T2w signal *(green arrow)*, when present, is diagnostic of VS over meningioma. Poor prognosticator for hearing preservation.
  - **Lateralised sigmoid sinus** - pre-operative planning for retrosigmoid approach.

What's new? Diffusion Tensor Imaging (DTI) for pre-operative planning

- Combines gradients of diffusion-weighted images to identify anisotropic diffusion in white-matter tracts
- Surgical concordance of 92% in VS >2.5cm
- ↓ intra-operative time and ↓ risk of facial nerve injury
- Failure rate 6%, associated with larger sized VS >3.5cm

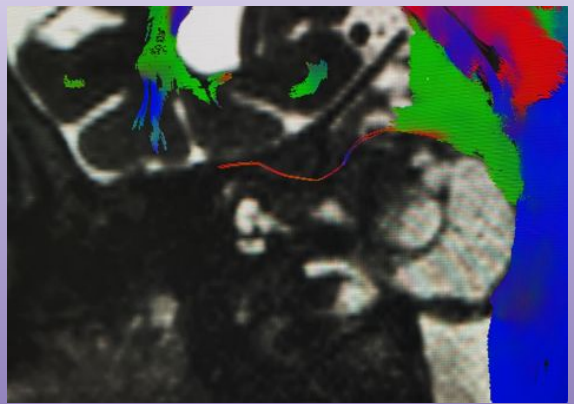

Fig 2. Coronal DTI mapping the course of the facial nerve (*red line*) in a patient with right VS.

Internal Acoustic Meatus (IAM) - continued

Meningioma
Second most common IAM neoplasm.
Eccentric to IAM with broad dural base, dural tail, and calcifications in 25%.
Absence of IAM expansion.

Fig 3. Left CPA meningioma.

Facial nerve schwannoma
<1% of temporal bone tumours. Mimics VS.
Most commonly at geniculate ganglion fossa, involving adjacent segments and expanding facial nerve canal *(yellow arrows)*.

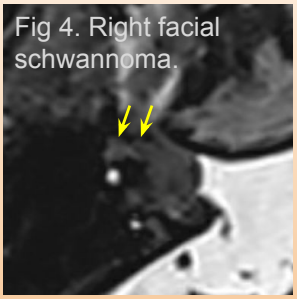

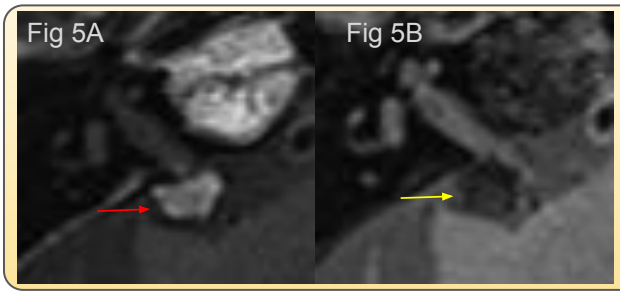

Lipoma
Extremely rare (0.1% of cerebellopontine angle [CPA] neoplasms). A mimicker of VS.

Fig 5. A right CPA lipoma showing high T1-weighted signal *(Fig 5A, red arrow)*, with suppression of signal on fat-suppressed image *(Fig 5B, yellow arrow)*.

Middle Ear and Mastoid

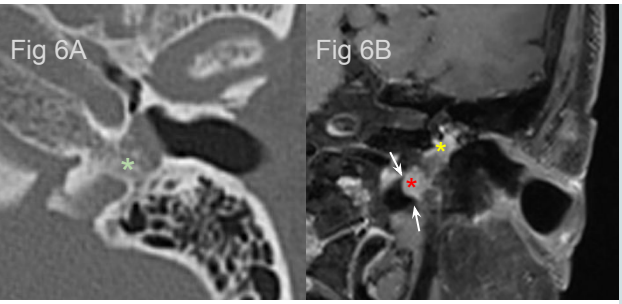

Fig 6A. Axial CT shows left middle ear soft tissue with permeative bone erosion *(green asterisk)*.
Fig 6B. Coronal T1-weighted post-contrast dark-blood images showing jugular *(red asterisk)* and tympanic *(yellow asterisk)* components of glomus jugulotympanicum. Note the vascular invasion to jugular bulb *(white arrows)*.

Head and neck paraganglioma (HNPGL)

- Mostly parasympathetic origin and non-functioning.
- 50% associated with germline mutation (↑risk multifocality).
- **Glomus tympanicum**: arises from Jacobsen nerve overlying cochlear promontory.
- **Glomus jugulotympanicum:** arising from the jugular foramen with permeative bone erosion (Fig 6A, *green asterisk*) extending to the middle ear.
- 'Salt and pepper' appearance on MRI (T1 bright haemorrhagic foci, T2 dark flow voids).
- **MR angiography (MRA)** - Contrast-enhanced MRA ↑ sensitivity and specificity for HNPGL to 100% and 94%, vs. contrast MRI alone (94% and 41%). Identifies tumour vascular supply for pre-operative embolisation.
- **Dark-blood imaging** - allows delineation of tumour extent from vascular structures (Fig 6B).

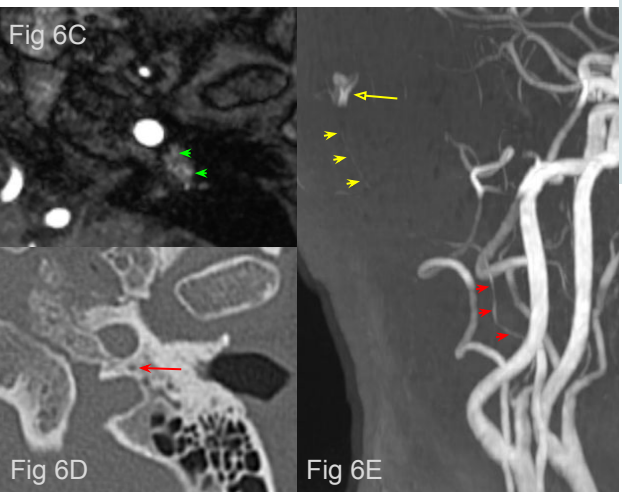

Fig 6C. Internal hyperintensities *(green arrowheads)* on non-contrast time-of-flight (TOF) MRA, confirming high flow.
Fig 6D. Asymmetrically enlarged inferior tympanic canaliculus *(red arrow)* housing the inferior tympanic artery, compared to contralateral side (not shown).
Fig 6E. Maximum-intensity projection time-of-flight MRA confirms arterial supply to glomus jugulotympanicum *(yellow arrow)* from the inferior tympanic artery *(yellow arrowheads)*, a branch of ascending pharyngeal artery *(red arrowheads)*.

Advanced MRI Techniques - Dynamic Contrast Enhanced (DCE) MRI

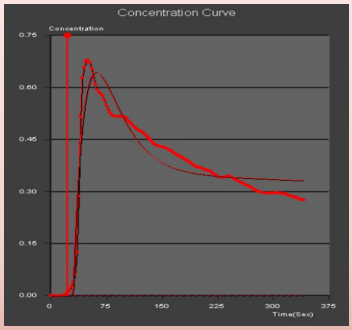

Paragangliomas show fast time-to-peak with rapid washout, along with low Ktrans values (transfer constant, reflecting capillary permeability and extravascular contrast leakage) and Kep (reflux rate, reflecting extravascular contrast returning to blood vessel).

For endolymphatic sac tumours, plateau-type pattern (fast time-to-peak, with washout <30%) has been described.

Fig 7. DCE curve of a glomus jugulotympanicum. Fast time-to-peak (<120 seconds) with washout (>30%).

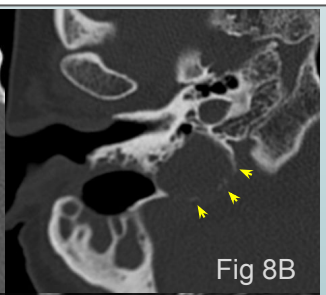

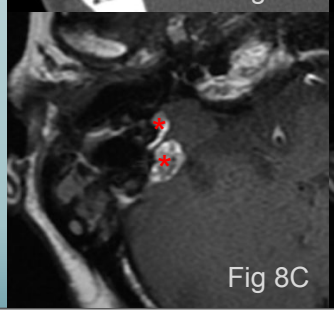

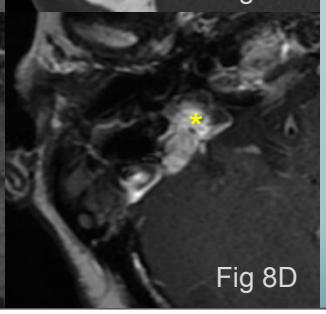

Endolymphatic sac tumour

Rare low-grade papillary adenocarcinoma, associated with von-Hippel Lindau syndrome.

Location: middle posterior margin of petrous bone, centred at vestibular aqueduct (which may be no longer seen).

CT: 'honeycomb' appearance of permeative bone erosion with bony spicules within (Fig 8A, *red arrowheads*). May show incomplete peripheral bony rim (Fig 8B, *yellow arrows*).

MRI: Peripheral intrinsic T1 hyperintense foci are characteristic (Fig 8C, *red asterisks)*, and heterogeneous enhancement (Fig 8D, *yellow asterisk*).

Middle ear adenomatous neuroendocrine tumour (MEANT)

Rare. Previously known as middle ear adenoma, carcinoid. Usually indolent behaviour, but with potential for regional and distant metastasis (cervical lymph nodes, liver, and bone).

MRI: T2 intermediate to hyperintense. Otherwise, variable T1 signal, variable enhancement, variable restricted diffusion.

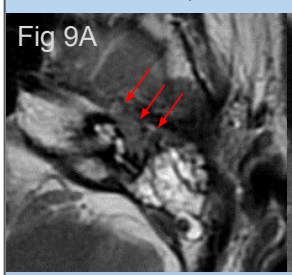

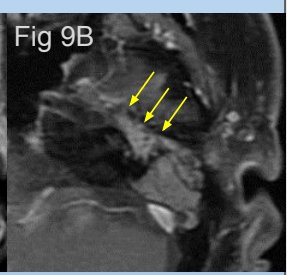

Fig 9. Left MEANT showing T2 intermediate signal (Fig 9A, *red arrows*), enhancing on T1 post-contrast images (Fig 9B, *yellow arrows*).

Radiation-induced sarcoma

Second-most common radiation-induced cancer, at 12% of cases (most common being squamous cell carcinoma).

- Location within the radiotherapy field, but away from the original tumour margin (vs recurrence).
- Except for osteosarcoma, imaging features are non-specific (rapidly growing destructive enhancing mass within prior radiotherapy field).

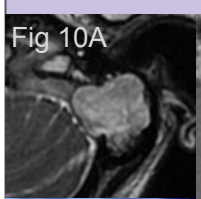

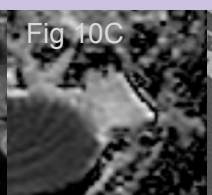

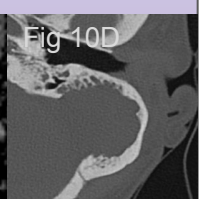

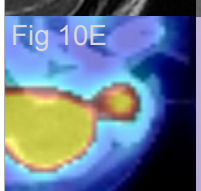

Fig 10. Left mastoid radiation-induced sarcoma showing T2 hyperintense signal (Fig 10A), enhancement (Fig 10B), facilitated diffusion on ADC map (Fig 10C), bone erosion (Fig 10D) and fluorodeoxyglucose (FDG) uptake (Fig 10E).

References:

1. Connor, Steve E J. “Imaging of the Vestibular Schwannoma: Diagnosis, Monitoring, and Treatment Planning.” *Neuroimaging clinics of North America* vol. 31,4 (2021): 451-471. doi:10.1016/j.nic.2021.05.006

2. Bubeníková, Adéla et al. “Application of diffusion tensor imaging of the facial nerve in preoperative planning for large vestibular schwannoma: a systematic review.” *Neurosurgical review* vol. 46,1 298. 11 Nov. 2023, doi:10.1007/s10143-023-02214-x

3. Savardekar, Amey R et al. “Preoperative diffusion tensor imaging-fiber tracking for facial nerve identification in vestibular schwannoma: a systematic review on its evolution and current status with a pooled data analysis of surgical concordance rates.” *Neurosurgical focus* vol. 44,3 (2018): E5. doi:10.3171/2017.12.FOCUS17672

4. Goldman, Matthew J et al. “Radiosurgery for Intracranial Meningiomas: A Review of Anatomical Challenges and an Update on the Evidence.” *Cancers* vol. 17,1 45. 27 Dec. 2024, doi:10.3390/cancers17010045

5. Mundada, Pravin et al. “Imaging of facial nerve schwannomas: diagnostic pearls and potential pitfalls.” *Diagnostic and interventional radiology (Ankara, Turkey)* vol. 22,1 (2016): 40-6. doi:10.5152/dir.2015.15060

6. You, Dan et al. “Clinical Predilection Features of Middle Ear Adenomatous Neuroendocrine Tumors: A Review of 10 Patients and a Special Case Is Attached.” *Ear, nose, & throat journal*, 1455613241264435. 8 Oct. 2024, doi:10.1177/01455613241264435

7. Engel, M S D et al. “Management and outcome of middle ear adenomatous neuroendocrine tumours: A systematic review.” *Oral oncology* vol. 121 (2021): 105465. doi:10.1016/j.oraloncology.2021.105465

8. King, A D et al. “Radiation induced sarcomas of the head and neck following radiotherapy for nasopharyngeal carcinoma.” *Clinical radiology* vol. 55,9 (2000): 684-9. doi:10.1053/crad.2000.0503

9. Thiagarajan, Anuradha, and N Gopalakrishna Iyer. “Radiation-induced sarcomas of the head and neck.” *World journal of clinical oncology* vol. 5,5 (2014): 973-81. doi:10.5306/wjco.v5.i5.973

10. Giannini, Lorenzo et al. “Radiation-Induced Sarcoma of the Head and Neck: A Review of the Literature.” *Frontiers in oncology* vol. 8 449. 17 Oct. 2018, doi:10.3389/fonc.2018.00449

11. Geng, Y et al. “Endolymphatic sac tumour: exploring the role of CT and MRI features in the diagnosis of 22 cases.” *Clinical radiology* vol. 77,8 (2022): e592-e598. doi:10.1016/j.crad.2022.04.010

12. Mathur, Ankit et al. “Imaging of skull base pathologies: Role of advanced magnetic resonance imaging techniques.” *The neuroradiology journal* vol. 28,4 (2015): 426-37. doi:10.1177/1971400915609341

13. Yuan, Ying et al. “Head and neck paragangliomas: diffusion weighted and dynamic contrast enhanced magnetic resonance imaging characteristics.” *BMC medical imaging* vol. 16 12. 1 Feb. 2016, doi:10.1186/s12880-016-0114-3

14. Lin, Edward P et al. “Head and Neck Paragangliomas: An Update on the Molecular Classification, State-of-the-Art Imaging, and Management Recommendations.” *Radiology. Imaging cancer* vol. 4,3 (2022): e210088. doi:10.1148/rycan.210088

15. Totten, Douglas J et al. “Cerebellopontine Angle and Internal Auditory Canal Lipomas: Case Series and Systematic Review.” *The Laryngoscope* vol. 131,9 (2021): 2081-2087. doi:10.1002/lary.29434